

ARBORESCENT LINKS AND MODULAR TAILS

ROBERT OSBURN AND MATTHIAS STORZER

ABSTRACT. We prove an explicit formula for the tail of the colored Jones polynomial for a class of arborescent links in terms of a product of theta functions and/or false theta functions. We also provide numerical evidence towards a classification of the modularity of tails of the colored Jones polynomial for alternating knots.

1. INTRODUCTION

Let K be a knot and $J_N(K; q)$ be the N th colored Jones polynomial, normalized to be 1 for the unknot and the classical Jones polynomial for $N = 2$. The colored Jones polynomial features prominently in many open problems in quantum topology. For example, the holy grail in this area is the Volume Conjecture [35, 42, 43, 45]. This conjecture relates the asymptotic behavior of $J_N(K; q)$ evaluated at an N th root of unity $\zeta_N := e^{\frac{2\pi i}{N}}$ to the simplicial volume (or Gromov norm) of the knot complement. Precisely,

$$\lim_{N \rightarrow \infty} \frac{\log |J_N(K; \zeta_N)|}{N} = \frac{\text{Vol}(S^3 \setminus K)}{2\pi} \quad (1.1)$$

for all knots K . One consequence of this conjecture is the following: if (1.1) is true, then a knot K is trivial if and only if all of its colored Jones polynomials $J_N(K; q)$ are trivial. The conjecture has been proven for the following knots and links [53]: torus knots, all hyperbolic knots with at most seven crossings, Borromean rings, twisted Whitehead links, Whitehead chains and, very recently, hyperbolic double twist knots [46]. In [57], Zagier formulated a generalization of (1.1) which also incorporated the quantum modularity of $J_N(K; q)$ for hyperbolic knots K . For recent work in this direction, see [9, 23, 24, 51].

In this paper, we are interested in stability properties for the coefficients of $J_N(L; q)$ where L is a link. The *tail* of the colored Jones polynomial of a link L (if it exists) is a power series $\Phi_L(q)$ whose first N coefficients agree (up to a common sign) with the first N coefficients of $J_N(L; q)$ for all $N \geq 1$. In 2006, Dasbach and Lin [15] conjectured that the tail exists for all alternating links L . This conjecture was first resolved by Armond [4] and then another proof and an explicit q -multisum expression for the tail of $J_N(L; q)$ was given in [21]. Subsequent intriguing developments include proving the existence (and non-existence) of the tail for families of knots and links [5, 6, 16–19, 27–29, 40, 41], the categorification of the tail [39, 48, 52], higher order stability [7, 30], higher rank tails [36, 54, 55] and connections to representation theory and vertex operator algebras [31–34].

Date: April 28, 2025.

2020 Mathematics Subject Classification. 57K10, 57K14, 57M15, 11F27.

Key words and phrases. Arborescent knots, tails, colored Jones polynomial, theta functions, false theta functions, asymptotics.

One can also find in [21] a table of forty-three conjectural identities between $\Phi_K(q)$ and products of theta functions and/or false theta functions, namely for a positive integer b , define

$$h_b = h_b(q) = \sum_{n \in \mathbb{Z}} \epsilon_b(n) q^{\frac{bn(n+1)}{2} - n}$$

where

$$\epsilon_b(n) = \begin{cases} (-1)^n & \text{if } b \text{ is odd,} \\ 1 & \text{if } b \text{ is even and } n \geq 0, \\ -1 & \text{if } b \text{ is even and } n < 0. \end{cases}$$

This table [21, Table 6] consists of all alternating knots up to 8_4 , the twist knots K_p , $p > 0$ or $p < 0$, the torus knots $T(2, p)$, $p > 0$, each of their mirror knots K^* and 8_5^* . For example, we have

$$\begin{aligned} \Phi_{5_2}(q) &= (q)_\infty^5 \sum_{a,b,c,d,e \geq 0} \frac{q^{2a^2+ac+ad+ae+b^2+be+cd+de+a+c+d+e}}{(q)_a(q)_{a+c}(q)_{a+d}(q)_{a+e}(q)_b(q)_{b+e}(q)_c(q)_d(q)_e} \\ &\stackrel{?}{=} h_4. \end{aligned} \tag{1.2}$$

Here and throughout, we use the standard q -Pochhammer symbol

$$(a)_n = (a; q)_n := \prod_{k=1}^n (1 - aq^{k-1}),$$

valid for $n \in \mathbb{N} \cup \{\infty\}$. Note that $h_1 = 0$, $h_2 = 1$ and $h_3 = (q)_\infty$. In general, h_b is a theta function if b is odd and a false theta function if b is even. The modularity in the former situation is classical [11] while false theta functions are only recently known as examples of quantum modular forms [25, Section 4.4]. Andrews [3] verified the conjecture for the knots 3_1 , 4_1 and 6_2 . In [37], Keilthy and the first author proved not only (1.2), but *all* of the remaining conjectural identities in [21] via a unified q -theoretic approach. This approach was then used in [8] to extend [21, Table 6] to all alternating knots up to ten crossings. Curiously, there are entries in [8, Tables 1 and 2] and [21, Table 6] in which a conjectural identity for $\Phi_K(q)$ is not known. Moreover, there is no known conjectural identity for *any* alternating knot (or its mirror) from 10_{79} to 10_{123} .

Our main goal in this paper is to prove an explicit formula for the tail of the colored Jones polynomial for a class of alternating links in terms of products of h_b 's. In order to state our main result, we require some setup. For further details, see Section 2. A weighted tree¹ $\Gamma = (\mathcal{V}, \mathcal{E}, w)$ is a finite planar tree with vertex set \mathcal{V} , edge set \mathcal{E} and weight $w(v) \in \mathbb{Z}$ associated to one section around $v \in \mathcal{V}$. Given Γ , one can associate a link L henceforth called an *arborescent link*. Γ is called *alternating* if there exists a bipartition $\mathcal{V}_+ \cup \mathcal{V}_-$ of \mathcal{V} with $\pm w(\mathcal{V}_\pm) \geq 0$. Here, $w(\mathcal{V}_+)$ (respectively, $w(\mathcal{V}_-)$) is the set of weights in \mathcal{V}_+ (respectively, \mathcal{V}_-). Note that Γ is alternating if we can choose a sign for each vertex of weight 0 such that the sets \mathcal{V}_\pm of vertices whose weights have sign \pm form a bipartition of \mathcal{V} . If Γ is alternating, then so is the corresponding link L . Our main result is now the following.

¹We assume that all weighted trees are reduced. See Remark 2.2 (ii).

Theorem 1.1. *Let $\Gamma = (\mathcal{V}, \mathcal{E}, w)$ be an alternating weighted tree with arborescent link L . If $0 \notin w(\mathcal{V}_-)$, then*

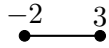
$$\Phi_L(q) = \prod_{v \in \mathcal{V}_+} h_{w(v)+e(v)} \quad (1.3)$$

where $e(v)$ is the number of edges adjacent to v .

Remark 1.2. Given a weighted tree Γ with arborescent link L , the mirror image L^* is constructed from the weighted tree obtained by flipping the signs of the weights of Γ . Thus, by Theorem 1.1, if $0 \notin w(\mathcal{V}_+)$, we have

$$\Phi_{L^*}(q) = \prod_{v \in \mathcal{V}_-} h_{-w(v)+e(v)}. \quad (1.4)$$

Remark 1.3. By Theorem 1.1 and Remark 1.2, one recovers *all* of the entries in [8, Tables 1 and 2] and [21, Table 6] without a “?”. For example, given the weighted tree



we will see in Section 2 that the associated knot is $K = 5_2$. By (1.3) and (1.4), we have

$$\Phi_{5_2}(q) = h_4, \quad \Phi_{5_2^*}(q) = h_3.$$

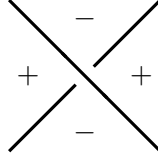
For the remaining arborescent knots K with “question marks”, the obstruction to finding an identity and thus determining the type of modularity for $\Phi_K(q)$ is the condition $0 \notin w(\mathcal{V}_-)$ in Theorem 1.1. This condition is equivalent to the fact that the reduced Tait graph of K is *not* the edge-connected sum of polygons (see Corollary 3.6). We discuss these cases further in Section 5.

The paper is organized as follows. In Section 2, we recall the construction of arborescent links as given in, e.g., [1, Chapter 17], [10, Chapter 12] or [20, Chapter 1]. In Section 3, we prove Theorem 1.1 using properties of reduced Tait graphs for arborescent links (in particular, see the key result Proposition 3.5 which is of independent interest). In Section 4, we give applications of Theorem 1.1 to various examples of arborescent knots. In Section 5, we discuss asymptotic properties of $\Phi_K(q)$ when Theorem 1.1 is not applicable. These asymptotics suggest a classification of alternating arborescent knots K such that $\Phi_K(q)$ is a product of h_b ’s (see Question 5.2).

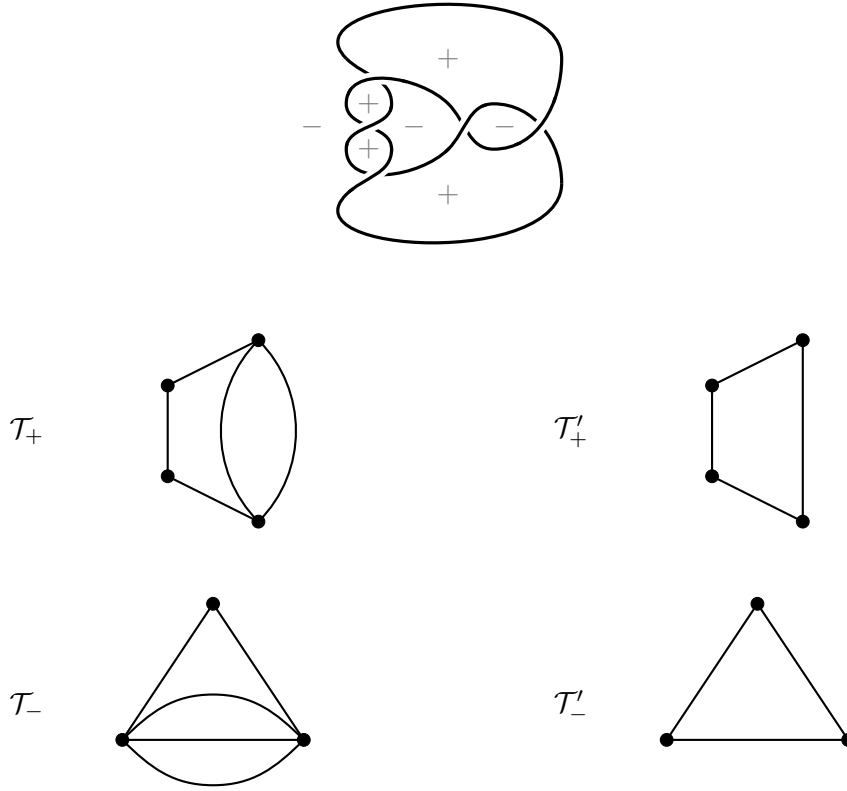
2. PRELIMINARIES

We begin by recalling some background from knot theory.

2.1. Tait graphs. Let L be an alternating link and D its associated *sign-colored* diagram which satisfies the rule in Figure 1 at each crossing of L . The \pm -Tait graphs \mathcal{T}_\pm of an alternating link with sign-colored diagram D are the graphs with vertices corresponding to the \pm -colored faces of D . Two vertices form an edge if the corresponding faces share a crossing. For a given alternating link, \mathcal{T}_+ is dual to \mathcal{T}_- . Moreover, the $+$ -Tait graph for L is the $-$ -Tait graph for the mirror L^* and vice versa. The *reduced* Tait graphs \mathcal{T}'_\pm are obtained from \mathcal{T}_\pm by replacing every set of two edges that connect the same two vertices by a single edge and removing loops.

FIGURE 1. $+$ and $-$ regions.

For example, a sign-colored diagram, Tait graphs and reduced Tait graphs for $K = 5_2$ are given in Figure 2.

FIGURE 2. Signed-colored diagram, \mathcal{T}_\pm and \mathcal{T}'_\pm for $K = 5_2$.

2.2. Arborescent links. Following [1, Chapter 17], [10, Chapter 12] or [20, Chapter 1], we introduce arborescent links which are a class of links associated to weighted trees. The construction of arborescent links described below is equivalent to that of Conway's algebraic links [14], see [10, Chapter 14.3] for a direct comparison.

Definition 2.1. A *weighted tree* $\Gamma = (\mathcal{V}, \mathcal{E}, w)$ is a planar embedding of a tree $(\mathcal{V}, \mathcal{E})$ together with a weight $w(v) \in \mathbb{Z}$ assigned to one section around v for each vertex $v \in \mathcal{V}$.

For a given weighted tree Γ , the weights are depicted as integers written in its sections. We now proceed as follows:

- (1) Let $v \in \mathcal{V}$ be a vertex with weight $w(v)$ and $n \in \mathbb{Z}_{\geq 0}$ adjacent vertices $v_1, \dots, v_n \in \mathcal{V}$ in counterclockwise order around v . We construct a ribbon associated to v that has n marked squares corresponding to v_i , $i = 1, \dots, n$, followed by $w(v)$ half-twists, see Figure 3. We use the convention that \times is a positive half-twist. The ribbon has two orientations: a horizontal core orientation (c) and a vertical normal orientation (n) .

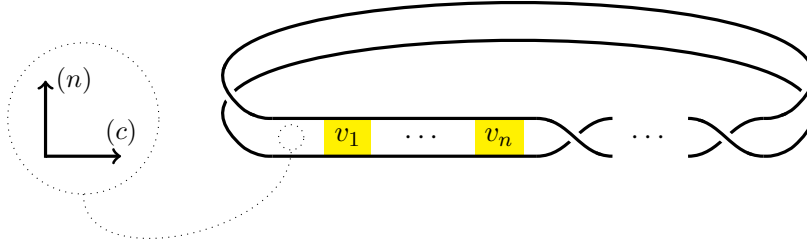


FIGURE 3. The ribbon associated to v .

- (2) For every edge $(v, v') \in \mathcal{E}$, we plumb the ribbons for v and v' along the squares for v' and v such that the core orientation of v matches the normal orientation of v' and vice versa.
- (3) The plumbed ribbons define a surface and the boundary of this surface is a link L . We say that L is the *arborescent link* associated to Γ .

Remark 2.2. (i) If Γ is alternating, then so is the arborescent link L by (1)–(3).

(ii) A weighted tree Γ is *reduced* if it has no vertex of degree at most 2 and weight 0. According to [1, Section 17.3 (0.2), Section 17.5.3], this condition ensures that any vertex with weight 0 and degree 2 can be removed from Γ without changing L and that L is prime and unsplittable. Throughout this paper, we assume (without further mention) that all weighted trees Γ are reduced.

We now illustrate this construction.

Example 2.3. (1) For the weighted tree in Figure 4, we construct the ribbons associated to the vertices v_1 and v_2 in Figure 5. Plumbing the two ribbons in Figure 5 yields the surface whose boundary can be transformed into the knot $K = 5_2$, see Figure 6.

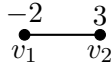


FIGURE 4. A weighted tree for 5_2 .

- (2) We consider the weighted tree in Figure 7. The ribbons corresponding to the vertices v_1 , v_2 and v_3 are given in Figure 8. Plumbing the three ribbons in Figure 8 leads to the surface whose boundary can be transformed into the knot $K = 8_5$, see Figure 9.

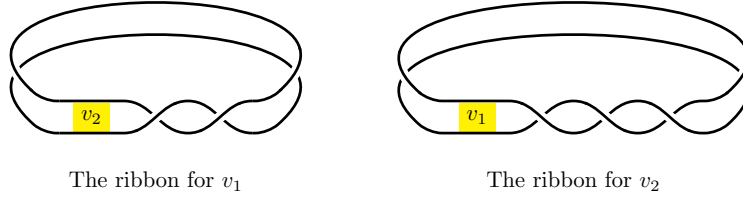


FIGURE 5. The two ribbons for Figure 4.

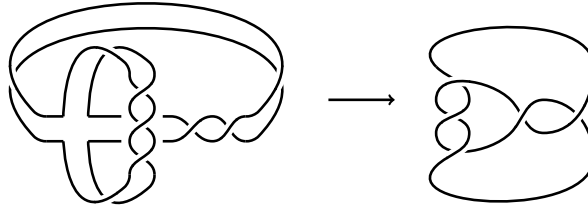
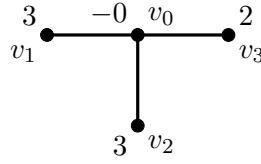
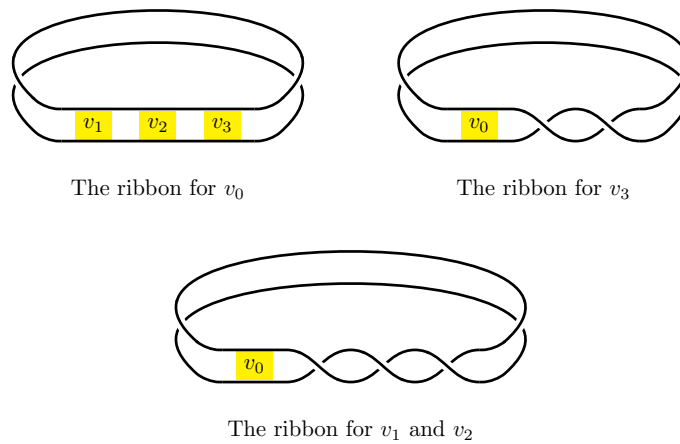
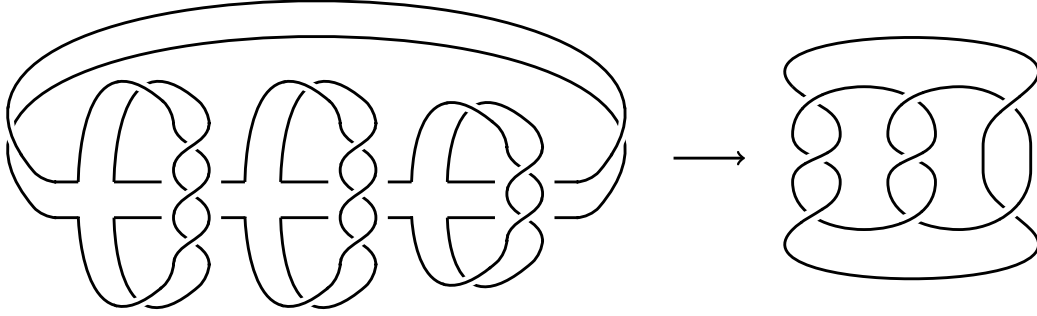
FIGURE 6. The surface for the two plumbed ribbons and 5_2 .FIGURE 7. A weighted tree for 8_5 .

FIGURE 8. The three ribbons for Figure 7.

FIGURE 9. The surface for the three plumbed ribbons and 8_5 .

2.3. Arborescent tangles. A tangle is defined as a region of a link diagram with exactly four emerging strings in the directions NW, NE, SE and SW. Two tangles are equivalent if one can be deformed into the other via a sequence of Reidemeister moves without changing the four emerging strings or moving another string over the emerging strings. A *weighted rooted tree* is a weighted tree with a marked vertex, the *root*, which has an emanating germ in one direction, here depicted by \bullet . For a weighted rooted tree with root v_0 , the associated weighted tree is the tree where v_0 is considered as an ordinary vertex. In this case, we define an *arborescent tangle* as the boundary of the surface corresponding to the associated weighted tree where the ribbon for v_0 is cut at the place corresponding to the germ, leaving four emanating strings. Consider the weighted tree from Example 2.3 (1) with root v_1 as in Figure 10. The corresponding tangle is given by Figure 11.

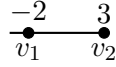
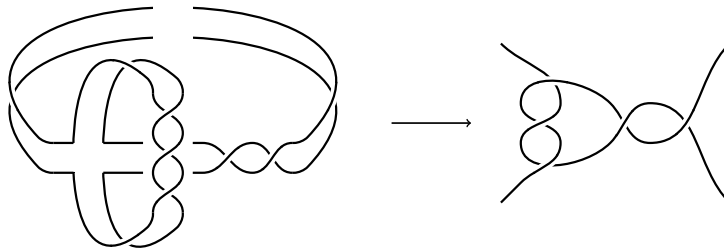
FIGURE 10. A weighted rooted tree for 5_2 .

FIGURE 11. The tangle for Figure 10.

We extend the notion of alternating from weighted trees to weighted rooted trees and adapt the bipartition $\mathcal{V} = \mathcal{V}_+ \cup \mathcal{V}_-$ accordingly. In this case, the corresponding tangle is alternating.

The closure of a tangle is the link L that is obtained by connecting the string in the NW direction with the one in the NE direction as well as the string in the SW direction with the

one in the SE direction. For example, the closure of the tangle in Figure 11 is the 5_2 knot as in Figure 6. The closure of an arborescent tangle is the arborescent link constructed from the associated weighted tree.

The \pm -Tait graphs \mathcal{T}_{\pm} for an alternating tangle are defined as in Section 2.1 with the addition of marked vertices corresponding to the North and South faces or the East and West faces. They are depicted by \otimes . The reduced Tait graphs \mathcal{T}'_{\pm} of a tangle are obtained from the Tait graphs \mathcal{T}_{\pm} of a tangle by replacing multiple edges with single edges and removing loops.

Remark 2.4. The (reduced) Tait graphs for the closure L of a tangle can be obtained from the (reduced) Tait graphs of the tangle as follows:² Assume that the North and South faces are colored by $\varepsilon \in \{+, -\}$ and thus the East and West faces are colored by $-\varepsilon$. Then the (reduced) ε -Tait graph of L can be obtained from the (reduced) vertical Tait graph of the tangle by unmarking the marked vertices. The (reduced) $-\varepsilon$ -Tait graph of L is formed by identifying the two marked vertices in the (reduced) horizontal Tait graph of a tangle. For example, for an arborescent tangle that is constructed from an alternating weighted rooted tree with root $v_0 \in \mathcal{V}_{-\varepsilon}$, the North and South faces are colored by ε .

Example 2.5. (1) Consider the tangle corresponding to the weighted rooted tree in Figure 12

$$\begin{array}{c} w(v) \\ \bullet \\ \text{---} \end{array}$$

FIGURE 12. A weighted rooted tree for a single vertex.

If $w(v) \neq 0$ and $\pm = \text{sign}(w(v))$, the Tait graphs \mathcal{T}_{\pm} and \mathcal{T}_{\mp} are given in Figure 13 with $|w(v)| + 1$ vertices (including the two marked vertices) and $|w(v)|$ edges, respectively.

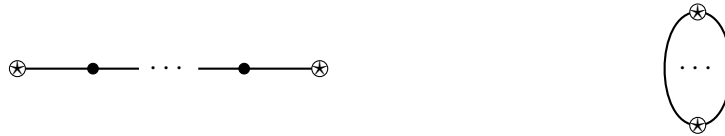


FIGURE 13. The Tait graphs \mathcal{T}_{\pm} (left) and \mathcal{T}_{\mp} (right) for Figure 12.

(2) The Tait graphs for the tangle in Figure 11 are given in Figure 14. From Figure 14, we obtain the Tait graphs for 5_2 as depicted in Figure 2 by unmarking the marked vertices for \mathcal{T}_{+} and identifying the marked vertices for \mathcal{T}_{-} .



FIGURE 14. The Tait graphs \mathcal{T}_{+} (left) and \mathcal{T}_{-} (right) for Figure 11.

²Here and throughout, for $\varepsilon \in \{+, -\}$, we write $-\varepsilon$ to mean the opposite choice of sign as for ε .

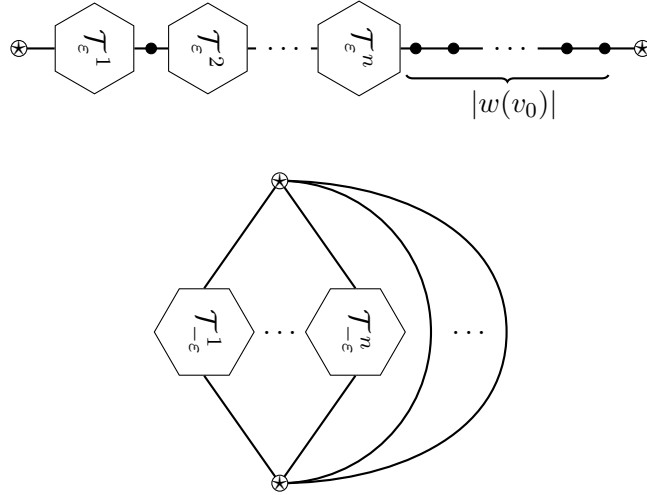
3. PROOF OF THEOREM 1.1

In order to prove Theorem 1.1, we need the following four results. We depict tangles T (with indices) by circles, weighted trees Γ (with indices) by squares and Tait graphs \mathcal{T} (with indices) by hexagons. We also denote North-South (respectively, East-West) Tait graphs with marked vertices as in Figure 15.



FIGURE 15. North-South (left) and East-West Tait (right) graphs.

Proposition 3.1. *Let Γ be an alternating weighted rooted tree with root v_0 and associated tangle T . Let $v_0 \in \mathcal{V}_\varepsilon$ be connected to the subgraphs $\Gamma_1, \dots, \Gamma_n$ via the vertices $v_1, \dots, v_n \in \mathcal{V}_{-\varepsilon}$ in counterclockwise order. Let \mathcal{T}_\pm^i denote the Tait graphs of the tangle corresponding to the tree Γ_i with root v_i for $i = 1, \dots, n$. Then the Tait graph \mathcal{T}_ε of Γ is given by Figure 16 (top) with $|w(v_0)| + 1$ additional vertices on the right, including the marked vertex. Moreover, the Tait graph $\mathcal{T}_{-\varepsilon}$ of Γ is given by Figure 16 (bottom) with $|w(v_0)|$ additional edges from the top vertex to the bottom vertex.*

FIGURE 16. The Tait graph \mathcal{T}_ε (top) and the Tait graph $\mathcal{T}_{-\varepsilon}$ (bottom).

Proof. By assumption, Γ has the shape as in Figure 17. Consider the ribbon corresponding to v_0 with gluing points for v_1, \dots, v_n followed by $w(v_0)$ half-twists. We assume that $v_0 \in \mathcal{V}_+$, i.e., $\varepsilon = +$ and $w(v_0) \geq 0$. A similar argument holds for $v_0 \in \mathcal{V}_-$. As Γ is alternating, $v_1, \dots, v_n \in \mathcal{V}_-$ and so $w(v_i) \leq 0$. Let T_i denote the tangle for Γ_i . Then the tangle associated to Γ_i with root v_i is in Figure 18. The tangle for Γ with root v_0 with marked squares for v_1, \dots, v_n is in Figure 19.

We then glue the tangles associated with v_1, \dots, v_n to the one for v_0 as in Section 2.2 and rearrange the strands to obtain the tangle for Γ , see Figure 20. Using Figure 1 and Remark 2.4, the Tait graphs \mathcal{T}_\pm for Figure 20 are of the shape in Figure 16. \square

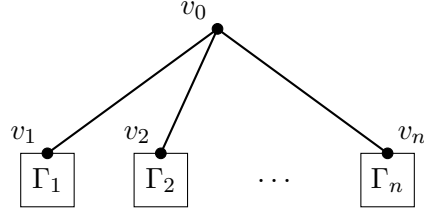


FIGURE 17. Γ with root v_0 .

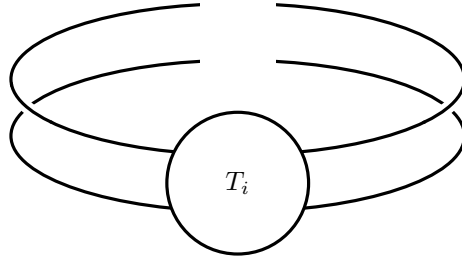


FIGURE 18. Tangle for Γ_i with root v_i .

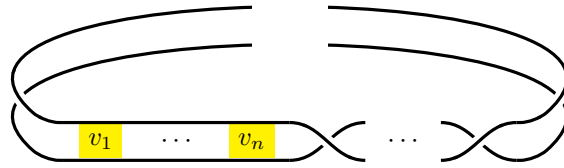


FIGURE 19. Tangle for Γ with root v_0 .

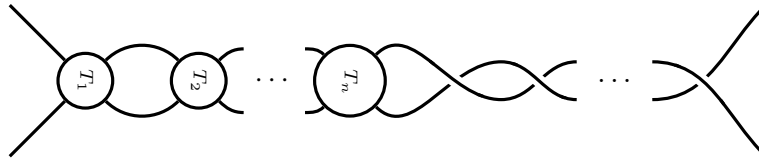


FIGURE 20. The tangle for Γ with root v_0 .

Example 3.2. According to Example 2.5 (1), the Tait graphs for $\overset{3}{-}\bullet$ are given in Figure 21. Proposition 3.1 implies that the Tait graphs for the rooted tree in Figure 10 are given in Figure 22 in accordance with Figure 14.



FIGURE 21. The Tait graphs \mathcal{T}_+^1 (left) and \mathcal{T}_-^1 (right) for the root $v_1 = 3$.

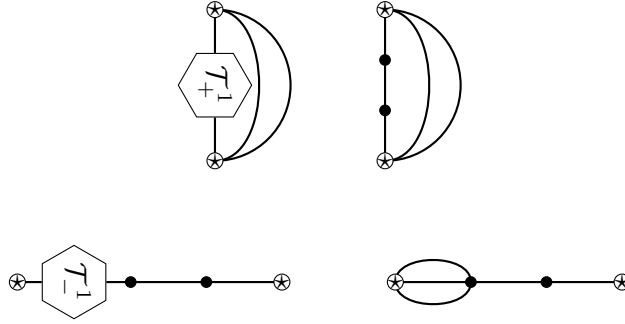


FIGURE 22. The Tait graphs \mathcal{T}_+ (top) and \mathcal{T}_- (bottom) for Figure 10.

Lemma 3.3. Let $\Gamma = (\mathcal{V}, \mathcal{E}, w)$ be an alternating weighted rooted tree with $|\mathcal{V}| \geq 2$ and root $v_0 \in \mathcal{V}_-$ as in Figure 23 with weighted subgraphs $\Gamma^{i,j}$ with roots $x_{i,j}$ and Tait graphs for the

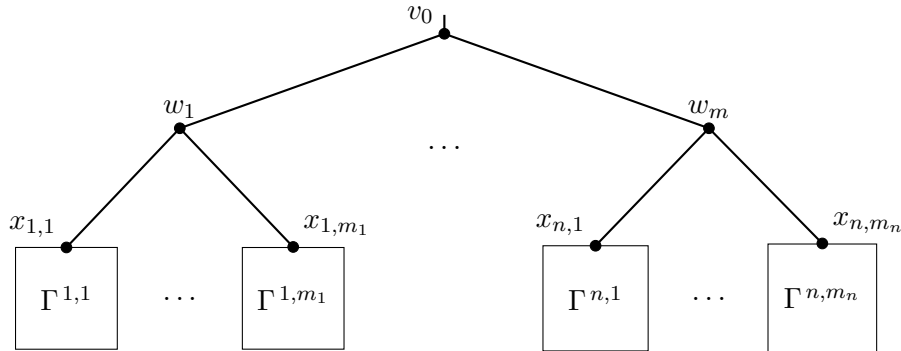
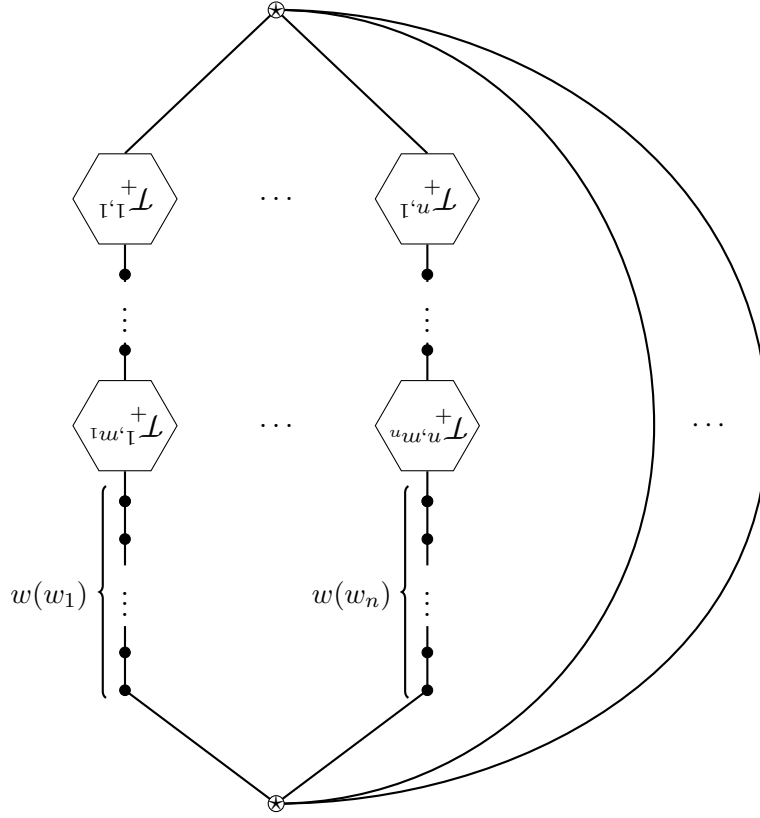
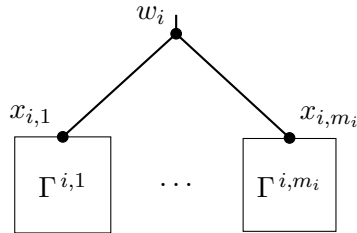


FIGURE 23. Γ with root $v_0 \in \mathcal{V}_-$.

corresponding tangles denoted by $\mathcal{T}_+^{i,j}$ for $i = 1, \dots, n$ and $j = 1, \dots, m_i$. Then the Tait graph for the tangle associated to Γ is given by Figure 24 with $|w(v_0)|$ edges from the top vertex to the bottom vertex and $w(w_i)$ additional vertices on the bottom of the i th string.

FIGURE 24. Tait graph for Γ .

Proof. Consider the weighted subtree with root w_i in Figure 25. By Proposition 3.1, the Tait graph \mathcal{T}_+^i corresponding to Figure 25 is given by Figure 26 where $\mathcal{T}_+^{i,j}$ are the Tait graphs for $\Gamma^{i,j}$ with roots $x_{i,j}$. We now apply Proposition 3.1 to Figure 23 and obtain that its Tait graph is given by Figure 27 with $|w(v_0)|$ edges between the top vertex and bottom vertex. Inserting Figure 26 into Figure 27 yields Figure 24. \square

FIGURE 25. Weighted subtree with root w_i .

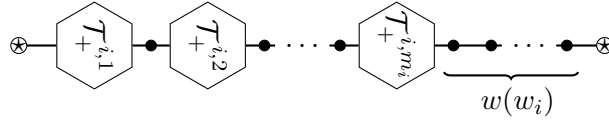
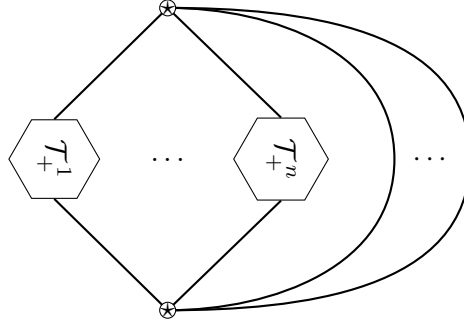
FIGURE 26. Tait graph \mathcal{T}_+^i for Figure 25.

FIGURE 27. Tait graph of Figure 23.

We say that a Tait graph (of a link or tangle) consists of *edge-connected polygons* if it can be built by gluing the polygons along a single edge.

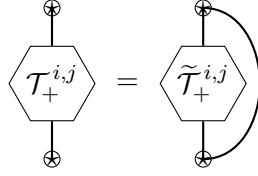
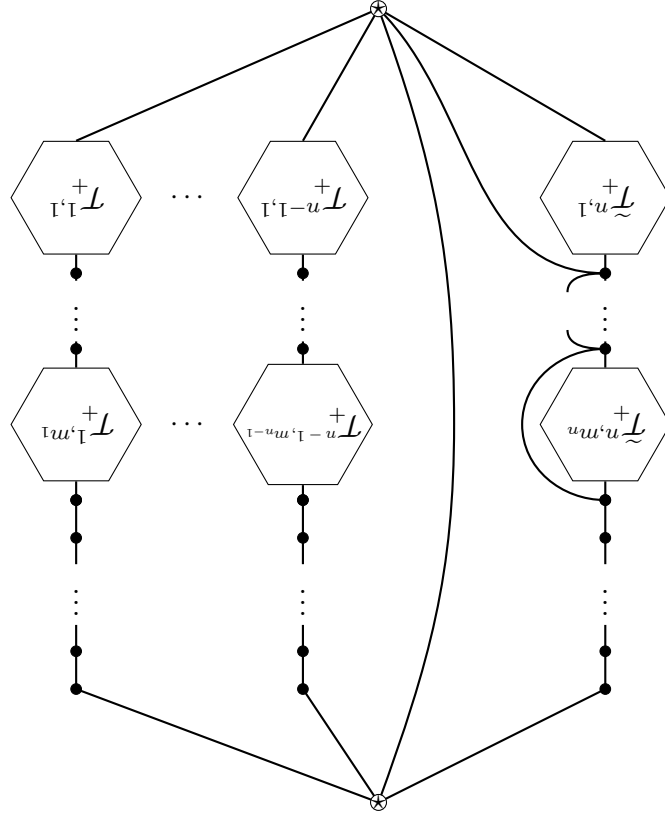
Lemma 3.4. *Let $\Gamma = (\mathcal{V}, \mathcal{E}, w)$ be an alternating weighted rooted tree with $|\mathcal{V}| \geq 2$, root $v_0 \in \mathcal{V}_-$ and $0 \notin w(\mathcal{V}_-)$. Then the reduced Tait graph \mathcal{T}'_+ of the tangle for Γ consists of edge-connected polygons of sizes $\{w(v) + e(v) : v \in \mathcal{V}_+\}$ and has an edge between the top vertex and bottom vertex.*

Proof. We proceed by induction on $|\mathcal{V}|$. Assume that $|\mathcal{V}| = 2$ with $\mathcal{V}_\pm = \{v_\pm\}$. As Γ has no leaf of weight 0 (see Remark 2.2), we have $w(v_+) \neq 0$. By Example 2.5 (1), \mathcal{T}'_+ is a polygon of size $w(v_+) + 1$.

Now assume that the claim is true for all Γ 's with less than $|\mathcal{V}|$ vertices. Let $v_0 \in \mathcal{V}_-$ be connected to $w_1, \dots, w_n \in \mathcal{V}_+$ and w_i be connected to the subgraphs $\Gamma^{i,j}$ (with vertices $\mathcal{V}_{i,j}$) via the vertices $x_{i,j} \in \mathcal{V}_-$ for $i = 1, \dots, n$ and $j = 1, \dots, m_i$ as in Figure 23. By abuse of notation, let $\mathcal{T}_+^{i,j}$ be the reduced Tait graphs for $\Gamma^{i,j}$ with roots $x_{i,j}$. With this notation, the reduced Tait graph \mathcal{T}'_+ is given as in Figure 24 with exactly one edge from the top vertex to the bottom vertex because $w(v_0) \neq 0$. By assumption, $\mathcal{T}_+^{i,j}$ consists of edge-connected polygons of sizes $\{w(v) + e(v) : v \in (\mathcal{V}_{i,j})_+\}$ and has an edge between the top and bottom vertices. We denote the reduced Tait graph $\mathcal{T}_+^{i,j}$ without this additional edge by $\tilde{\mathcal{T}}_+^{i,j}$ as depicted in Figure 28.

If we replace the Tait graphs $\mathcal{T}_+^{n,j}$ by $\tilde{\mathcal{T}}_+^{n,j}$ for $j = 1, \dots, m_n$ in Figure 24 and move the exterior edge across the rightmost string (consisting of the Tait graphs $\tilde{\mathcal{T}}_+^{n,j}$ for $j = 1, \dots, m_n$ and the vertices below them), then \mathcal{T}'_+ is given as in Figure 29. The edge from the top vertex to the bottom vertex in Figure 29 separates edge-connected polygons of sizes

$$\{w(w_n) + m_n\} \cup \bigcup_{j=1}^{m_n} \{w(v) + e(v) : v \in (\mathcal{V}_{n,j})_+\}$$

FIGURE 28. $\mathcal{T}_+^{i,j}$ (left) and $\tilde{\mathcal{T}}_+^{i,j}$ (right).FIGURE 29. The reduced Tait graph \mathcal{T}'_+ of the tangle for Γ .

on the right from the rest. If we apply the same procedure to the remaining strings on the left, we obtain that \mathcal{T}'_+ consists of edge-connected polygons of sizes

$$\bigcup_{i=1}^n \bigcup_{j=1}^{m_i} \{w(v) + e(v) : v \in (\mathcal{V}_{i,j})_+\} \cup \bigcup_{i=1}^n \{w(w_i) + m_i\} = \{w(v) + e(v) : v \in \mathcal{V}_+\}$$

since $m_i = e(w_i)$. □

Proposition 3.5. *Let Γ and L be as in Theorem 1.1 and assume that $|\mathcal{V}| \geq 2$. Then the reduced Tait graph \mathcal{T}_+ of L consists of edge-connected polygons of sizes $w(v) + e(v)$ where $v \in \mathcal{V}_+$.*

Proof. Choose $v_0 \in \mathcal{V}_-$ and consider the alternating weighted rooted tree Γ with root v_0 . By Lemma 3.4, the reduced $+$ -Tait graph for Γ consist of edge-connected polygons of sizes $\{w(v) + e(v) : v \in \mathcal{V}_+\}$ which agrees with the Tait graph \mathcal{T}_+ of L after unmarking the marked vertices, cf. Remark 2.4. \square

For our discussion in Section 5, we prove the following result.

Corollary 3.6. *Let Γ be an alternating weighted tree with arborescent link L and Tait graph \mathcal{T}_+ of L . Then \mathcal{T}_+ is not the edge-connected sum of polygons if and only if $0 \in w(\mathcal{V}_-)$.*

Proof. If $0 \notin w(\mathcal{V}_-)$, then Proposition 3.5 implies that \mathcal{T}_+ consists of edge-connected polygons. Conversely, if $v_0 \in \mathcal{V}_-$ with $w(v_0) = 0$, then Lemma 3.3 implies that the Tait graph \mathcal{T}_+ of Γ with root v_0 is given as in Figure 24 without an edge from the top vertex to bottom vertex because $w(v_0) = 0$. By Remark 2.2 (ii), the degree of v_0 is greater than 2. Thus, \mathcal{T}_+ is not the edge-connected sum of polygons because none of the edges drawn in Figure 24 decomposes \mathcal{T}_+ into polygons. \square

We are now in a position to prove our main result.

Proof of Theorem 1.1. Let $m \in \mathbb{N}$. Let L be an alternating link such that its reduced Tait graph \mathcal{T}'_+ consists of m edge-connected polygons of sizes $b_i \geq 2$, $i = 1, \dots, m$. According to [5, Theorem 2], $\Phi_L(q)$ is uniquely determined by \mathcal{T}'_+ . From [5, Theorem 5.1], we have

$$\Phi_L(q) = \prod_{i=1}^m h_{b_i}. \quad (3.1)$$

The result now follows from Proposition 3.5 and (3.1). \square

4. APPLICATIONS OF THEOREM 1.1

In this section, we give some consequences of Theorem 1.1. Since arborescent links are the same as algebraic links, the subsequent results are presented using Conway's notation [13].

4.1. 2-bridge knots. A 2-bridge knot (or rational knot) K can be constructed from a weighted tree given in Figure 30 for $d_1, \dots, d_n \in \mathbb{Z}_{>0}$. The Conway notation for K is $[d_n \dots d_1]$. Here,

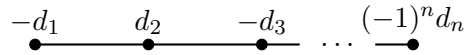


FIGURE 30. A weighted tree for 2-bridge knots.

the vertices v_j have weights d_j . We partition the vertices into the sets $\mathcal{V}_+ = \{v_j : j \text{ even}\}$ and $\mathcal{V}_- = \{v_j : j \text{ odd}\}$. We have $e(v_j) = 1$ if $j = 1$ or n and $e(v_j) = 2$ otherwise. With the vector

$$(b_1, \dots, b_n) := (d_1 + e(v_1), \dots, d_n + e(v_n)),$$

Theorem 1.1 immediately implies the following result.

Corollary 4.1. *If K is a 2-bridge knot as above, then*

$$\Phi_K(q) = \prod_{\substack{j=1 \\ j \text{ even}}}^n h_{b_j}, \quad \Phi_{K^*}(q) = \prod_{\substack{j=1 \\ j \text{ odd}}}^n h_{b_j}.$$

Example 4.2. (1) In Example 2.3 (1), the knot $K = 5_2$ was constructed from the weighted tree given in Figure 4. Thus, the Conway notation is $[3\ 2]$ and so by Corollary 4.1, we have

$$\Phi_{5_2}(q) = h_4, \quad \Phi_{5_2^*}(q) = h_3. \quad (4.1)$$

Equation (4.1) also follows from (3.1) and the Tait graphs of $K = 5_2$ given in Figure 2.

(2) Let $K = 7_4$ which has Conway notation $[3\ 1\ 3]$. An associated weighted tree is given by Figure 31 and so by Corollary 4.1, we have

$$\Phi_{7_4}(q) = h_3, \quad \Phi_{7_4^*}(q) = h_4^2. \quad (4.2)$$

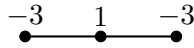


FIGURE 31. A weighted tree for 7_4 .

The reduced Tait graphs \mathcal{T}'_{\pm} of $K = 7_4$ are given in Figure 32 and so (4.2) also follows from (3.1).

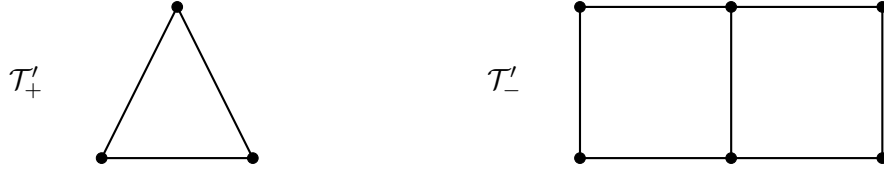


FIGURE 32. The reduced Tait graphs for 7_4 .

4.2. Montesinos knots. A *Montesinos knot* K can be constructed by a star-shaped weighted tree [1, Section 17.6.2] as in Figure 33 with center $k \in \mathbb{Z}_{\geq 0}$, $m \in \mathbb{Z}_{\geq 1}$ rays of length $n_i \in \mathbb{Z}_{\geq 1}$ and $d_1^{(i)}, d_2^{(i)}, \dots, d_{n_i}^{(i)} \in \mathbb{Z}_{\geq 1}$ for $i = 1, \dots, m$. The Conway notation for K is

$$[\mathbf{d}^{(1)}; \mathbf{d}^{(2)}; \dots; \mathbf{d}^{(m)+k}]$$

where $+^k$ means k copies of $+$ and $\mathbf{d}^{(i)}$ denotes the concatenation of the entries in the i th ray. For $v \in \mathcal{V}$, we have

$$e(v) = \begin{cases} m & \text{if } v \text{ is the center,} \\ 1 & \text{if } v \text{ is a leaf,} \\ 2 & \text{otherwise.} \end{cases}$$

For $i = 1, \dots, m$ and $j = 1, \dots, n_i$, define

$$b_j^{(i)} = d_{n_j}^{(i)} + e(v_{i,n_j})$$

where v_{i,n_j} is the j th vertex in the i th ray. Another application of Theorem 1.1 is the following.

Corollary 4.3. *If K is a Montesinos knot as above, then*

$$\Phi_{K^*}(q) = h_{m+k} \prod_{i=1}^m \prod_{\substack{j=1 \\ j \text{ even}}}^{n_i} h_{b_j^{(i)}}$$

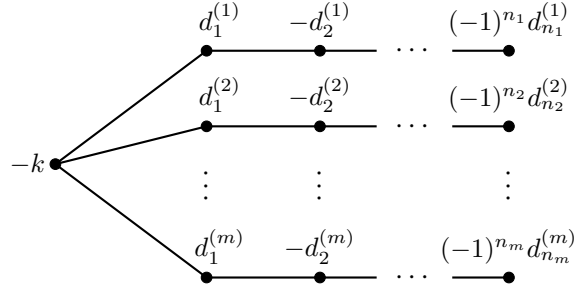


FIGURE 33. A weighted tree for Montesinos knots.

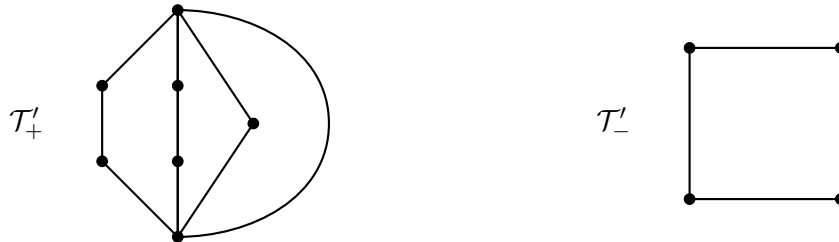
and, if $k \neq 0$,

$$\Phi_K(q) = \prod_{i=1}^m \prod_{\substack{j=1 \\ j \text{ odd}}}^{n_i} h_{b_j^{(i)}}.$$

Example 4.4. Consider the Montesinos knot $K = 9_{16}$ which has Conway notation $[3; 3; 2+]$. A weighted tree and diagram for 9_{16} are given in Figure 34. By Corollary 4.3, we have

$$\Phi_{9_{16}}(q) = h_4^2 h_3, \quad \Phi_{9_{16}^*} = h_4. \quad (4.3)$$

The reduced Tait graphs of 9_{16} are given in Figure 35 and so (4.3) also follows from (3.1).

FIGURE 34. A weighted tree and diagram for 9_{16} .FIGURE 35. The reduced Tait graphs for 9_{16} .

4.3. A non-Montesinos knot. Lastly, we consider the knot $K = 11a_{250}$ which has Conway notation $[(3; 2)1(3; 2)]$ and is not a Montesinos knot. A weighted tree [13, p. 38] and diagram for $11a_{250}$ are given in Figure 36. Hence, Theorem 1.1 is only applicable to $11a_{250}^*$. Thus, we have

$$\Phi_{11a_{250}^*}(q) = h_3^2. \quad (4.4)$$

The reduced Tait graphs of $11a_{250}$ are given in Figure 37 and so (4.4) also follows from (3.1).

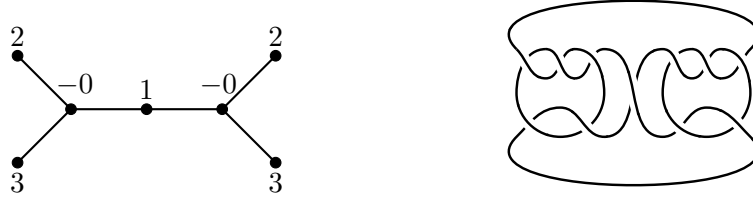


FIGURE 36. A weighted tree and diagram for $11a_{250}$.

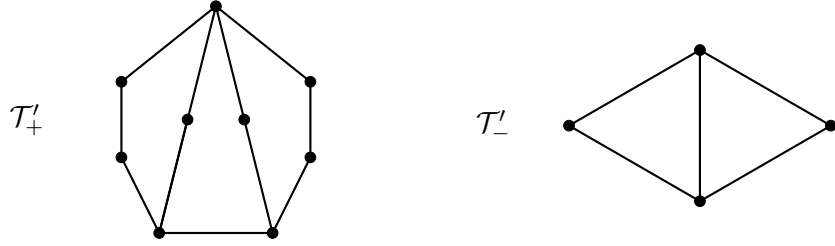


FIGURE 37. The reduced Tait graphs for $11a_{250}$.

5. ASYMPTOTICS OF $\Phi_K(q)$

The first arborescent knot for which Theorem 1.1 is not applicable is 8_5 . This knot is the first case in a family of pretzel knots for which Theorem 1.1 does not apply. The first non-arborescent knot is 8_{18} . In this section, we provide numerical evidence that the tail in these situations cannot be written as a product of the functions $h_b = h_b(q)$ and, more generally, is not a classical modular form, quasimodular form or mock modular form. This leads to the question of the classification of alternating knots K such that $\Phi_K(q)$ can be written as a product of h_b 's, see Question 5.2 and Remark 5.3.

We first compare the asymptotics of $h_b(e^{-h})$ as $h \rightarrow 0$ with the asymptotics of $\Phi_K(e^{-h})$ for a given knot K . This is motivated by a similar approach for the classification of modular Nahm sums [12, 47, 49, 50, 56]. As $h \rightarrow 0$ on a ray in the right half-plane, we have

$$h_b(e^{-h}) = \begin{cases} e^{-\pi^2/2bh} \sqrt{\frac{2\pi}{bh}} (\cos(2\pi(\frac{1}{4} - \frac{1}{2b})) + O(h)) & \text{if } b \text{ is odd,} \\ \frac{2}{b} + O(h) & \text{if } b \text{ is even.} \end{cases} \quad (5.1)$$

The computation (5.1) follows from the usual modular transformation of h_b if b is odd and from [38, Proposition, p. 98] if b is even. In both cases, we have $\lim_{h \rightarrow 0} h \log(h_b(e^{-h})) \in \pi^2 \mathbb{Q}$.

Hence, if a q -series f with asymptotics $h \log(f(e^{-h})) \rightarrow V$ as $h \rightarrow 0$ for some $V \in \mathbb{C}$ can be written as a product of h_b 's, the asymptotics in (5.1) imply that $V \in \pi^2\mathbb{Q}$. Although this condition cannot be verified numerically, computations can suggest if $V \in \pi^2\mathbb{Q}$ is likely.

Remark 5.1. A similar argument can be used to (numerically) exclude other modular behavior. If g is a modular form of integer (or half-integer) weight for some subgroup of $\mathrm{SL}_2(\mathbb{Z})$ of finite index, then its modular transformation implies that

$$h \log(g(e^{-h})) \rightarrow V \quad (5.2)$$

as $h \rightarrow 0$ on a ray in the right half-plane for some $V \in \pi^2\mathbb{Q}$, see [50, Lemma 3.1]. The same proof is also applicable to quasimodular forms (and mock modular forms) because they (their completions) have a similar transformation under $S = \begin{pmatrix} 0 & -1 \\ 1 & 0 \end{pmatrix}$. Therefore, if a q -series f has an asymptotic as in (5.2), $V \notin \pi^2\mathbb{Q}$ would also exclude these modular behaviors of $q^c f(q)$ for any $c \in \mathbb{Q}$.

5.1. Pretzel knots. A pretzel knot $P(d_1, \dots, d_n)$ with integers $d_i \geq 2$ for $i = 1, \dots, n$ is an arborescent knot associated with a star-shaped weighted tree, i.e., a Montesinos knot with center 0 and n rays of length one where the leaves have weight d_1, \dots, d_n , see Figure 38.

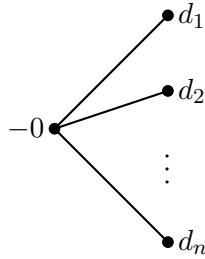


FIGURE 38. A weighted tree for $P(d_1, \dots, d_n)$.

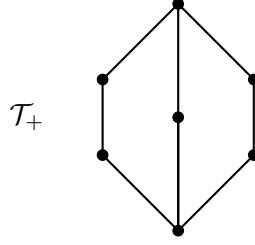
Here, Theorem 1.1 is not applicable. The tail of the colored Jones polynomial for pretzel knots of the form $K = P(2k + 1, 2u + 1, 2)$ for $k, u \in \mathbb{Z}_{\geq 1}$ has been computed explicitly. Recall that the q -binomial coefficient is given by

$$\begin{bmatrix} n \\ k \end{bmatrix} := \frac{(q)_n}{(q)_k (q)_{n-k}}.$$

By [16, Theorem 3.1], we have

$$\Phi_K(q) = (q)_\infty^2 \sum_{l_1 \geq 0} \cdots \sum_{l_k \geq 0} \sum_{p_1 \geq 0} \cdots \sum_{p_u \geq 0} \frac{q^{L_1^2 + \cdots + L_k^2 + L_1 + \cdots + L_k}}{(q)_{l_1} \cdots (q)_{l_k}} \frac{q^{P_1^2 + \cdots + P_u^2 + P_1 + \cdots + P_u}}{(q)_{p_1} \cdots (q)_{p_u}} \begin{bmatrix} l_k + p_u \\ p_u \end{bmatrix} \quad (5.3)$$

where $L_j = l_j + \cdots + l_k$ for $j = 1, \dots, k$ and $P_j = p_j + \cdots + p_u$ for $j = 1, \dots, u$. As discussed in Example 2.3 (2), $K = 8_5$ can be constructed from the weighted tree given in Figure 9. In particular, note that Theorem 1.1 is not applicable as $0 \in w(\mathcal{V}_-)$. The Tait graph \mathcal{T}_+ of $K = 8_5$ is given in Figure 39 and thus (3.1) is also not applicable.

FIGURE 39. \mathcal{T}_+ for 8_5 .

Observe that $K = 8_5 = P(3, 3, 2)$ (see Figure 9) and so (5.3) implies

$$\begin{aligned} \Phi_{8_5}(q) &= (q)_\infty^2 \sum_{a,b \geq 0} \frac{q^{a^2+a+b^2+b}}{(q)_a(q)_b} \begin{bmatrix} a+b \\ b \end{bmatrix} \\ &= 1 - 2q + q^2 - 2q^4 + 3q^5 - 3q^8 + q^9 + O(q^{10}). \end{aligned} \quad (5.4)$$

By comparing the first two coefficients, we see $\Phi_{8_5}(q) \neq h_4^2 h_3$ in contrast to Theorem 1.1. As $h \searrow 0$ and $q = e^{-h} \nearrow 1$, numerics suggest that we have

$$h \log(\Phi_{8_5}(e^{-h})) \rightarrow V_1 \quad (5.5)$$

where, with $X_1 \approx 0.5436890$ a root of $x^3 + x^2 + x - 1$,

$$\begin{aligned} V_1 &= -4 \operatorname{Li}_2(X_1) + \operatorname{Li}_2(X_1^2) - 2 \log(X_1)^2 + \frac{\pi^2}{6} \\ &= -1.352936859 \dots \end{aligned}$$

Here, Li_2 is the dilogarithm function [56]. Although we do not address it here, we note that (5.5) can potentially be proven using the techniques in [22, 50, 56]. Computing V_1 to a higher precision, it seems unlikely that $V_1 \in \pi^2 \mathbb{Q}$ is true. This suggests that $q^c \Phi_{8_5}(q)$ for any $c \in \mathbb{Q}$ cannot be written as a product of h_b 's and, more generally, is not modular as in Remark 5.1. If $h \rightarrow 0$ on a fixed ray in the right half-plane with $\arg h = .45\pi$, then the limit is even more convincing: numerics suggest that we have

$$h \log(\Phi_{8_5}(e^{-h})) \rightarrow V_2 \quad (5.6)$$

where, with $X_2 \approx -0.7718445 - 1.115143i$ a root of $x^3 + x^2 + x - 1$,

$$\begin{aligned} V_2 &= -4 \operatorname{Li}_2(X_2) + \operatorname{Li}_2(X_2^2) - 2 \log(X_2)^2 - 4\pi i \log(X) + \frac{\pi^2}{6} \\ &= -14.12794 \dots + 3.177293 \dots i, \end{aligned} \quad (5.7)$$

and $V_2 \notin \pi^2 \mathbb{Q}$.

In view of (3.1), the following phenomenon seems to relate the Tait graph \mathcal{T}_+ of $K = 8_5$ to the double-sum in (5.4). The Tait graph \mathcal{T}_+ of $K = 8_5$ consists of two 5-gons that are *not* edge-connected. If they were, then $\Phi_{8_5}(q)$ would equal h_5^2 by (3.1) and $\Phi_{8_5}(q)$ is *almost* given by h_5^2 , namely if $\begin{bmatrix} a+b \\ b \end{bmatrix}$ was not present in (5.4), then the resulting q -series would equal h_5^2 by the second Rogers-Ramanujan identity.

Similar computations have been performed for pretzel knots $K = P(2k + 1, 2u + 1, 2)$ with $k, u \leq 5$ using (5.3). These computations suggest that for all of these pretzel knots we have $h \log(\Phi_K(e^{-h})) \rightarrow V$ as $h \rightarrow 0$ for some $V \notin \pi^2 \mathbb{Q}$. Therefore, we suspect that $\Phi_K(q)$ for these knots K cannot be written as a product of h_b 's. Moreover, the Tait graph of K consists of two polygons of size $2k + 1$ and $2u + 1$, respectively. Finally, if $\begin{bmatrix} l_k + p_u \\ p_u \end{bmatrix}$ is removed from (5.3), the resulting q -series would equal $h_{2k+1} h_{2u+1}$ by the Andrews-Gordon identities [2].

5.2. The 8_{18} knot. We also discuss the modularity of $\Phi_K(q)$ for the first non-arborescent knot $K = 8_{18}$ [13, 14]. Although $K = 8_{18}$ cannot be constructed from a weighted tree, it does arise from the weighted graph [13, p. 151] given in Figure 40. The Tait graphs of $K = 8_{18}$ are given in Figure 41 and thus (3.1) is not applicable.



FIGURE 40. A weighted graph and diagram for 8_{18} .

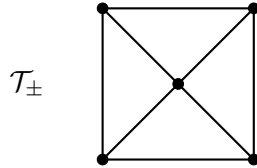


FIGURE 41. The Tait graphs for 8_{18} .

Using the algorithm from [21] and an elementary (yet lengthy) calculation, we have

$$\begin{aligned} \Phi_{8_{18}}(q) &= (q)_\infty^2 \sum_{a,b \geq 0} (-1)^{a+b} \frac{q^{\frac{1}{2}a(a+1) + \frac{1}{2}b(b+1)}}{(q)_a (q)_b} \begin{bmatrix} a+b \\ b \end{bmatrix} \\ &= 1 - 4q + 2q^2 + 9q^3 - 5q^4 - 8q^5 - 14q^6 + 10q^7 + 21q^8 + 14q^9 + O(q^{10}). \end{aligned} \quad (5.8)$$

From the first four coefficients, we see that $\Phi_{8_{18}}(q) \neq h_3^4$ in contrast to Theorem 1.1. Similar to 8_5 , we can compute the asymptotics of $\Phi_{8_{18}}(q)$ numerically. As $h \searrow 0$ on the real axis, it appears that $h \log(\Phi_{8_{18}}(e^{-h})) \rightarrow \frac{\pi^2}{3}$ which matches the asymptotics of a modular q -series. In fact, it has the same leading asymptotics as h_3^4 (which is the suggested formula for $\Phi_{8_{18}}(q)$ from Theorem 1.1 if it was applicable). However, if we instead consider the limit as $h \rightarrow 0$ with $\arg h = .45\pi$, then according to numerics

$$h \log(\Phi_{8_{18}}(e^{-h})) \rightarrow V_2 \quad (5.9)$$

where

$$V_2 = -\frac{\pi^2}{2} + 4 \operatorname{Li}_2(i) = -5.757269 \cdots + 3.663862 \cdots i. \quad (5.10)$$

This suggests that $\Phi_{8_{18}}(q)$ cannot be a product of h_b 's as $V_2 \notin \pi^2 \mathbb{Q}$. The Tait graphs \mathcal{T}_{\pm} of $K = 8_{18}$ in Figure 41 consist of four triangles and if $\begin{bmatrix} a+b \\ b \end{bmatrix}$ was absent in (5.8), then the resulting q -series equals $h_3^4 = (q)_{\infty}^4$ (which would be consistent with (3.1) if it was applicable).

5.3. Questions and outlook. The numerical observations in Section 5.1 suggest the following question.

Question 5.2. For an alternating arborescent knot K as in Theorem 1.1, are the following equivalent:

- (i) $0 \notin w(\mathcal{V}_-)$,
- (ii) The \pm -Tait graph of K is the edge-connected sum of polygons,
- (iii) $\Phi_K(q)$ is a product of h_b 's.

Remark 5.3. By Corollary 3.6, (i) and (ii) of Question 5.2 are equivalent. Moreover, by Theorem 1.1 and (3.1), either (i) or (ii) implies (iii). Clearly, it would be beneficial to consider more examples, e.g., [26]. In view of Section 5.2, one could hazard the following: for *any* alternating knot K , (ii) and (iii) are equivalent to the fact that K is an arborescent knot as in Theorem 1.1 with $0 \notin w(\mathcal{V}_-)$.

Finally, it would be desirable to understand the topological meaning of the (non)-modularity of $\Phi_K(q)$. Note that the limits in (5.6) and (5.9) for 8_5 and 8_{18} , respectively, can be rewritten as

$$\lim_{N \rightarrow \infty} \frac{\log(\Phi_K(e^{2\pi i/N}))}{N} = \frac{iV}{2\pi} \quad (5.11)$$

where $\frac{1}{N} \rightarrow 0$ along a ray in the upper half-plane. Because $\Phi_K(q) = \lim_N q^{c_N} J_N(K, q)$ for some factor c_N that is quadratic in N , equation (5.11) resembles the complexified Volume Conjecture [44]. This suggests that V as in (5.7) and (5.10) could be related to hyperbolic properties of K . This will be investigated in future work.

ACKNOWLEDGEMENTS

The first author is grateful to the Max-Planck-Institut für Mathematik for their hospitality and support as this work began during his stay from May 1-31, 2023. The second author would like to thank Stavros Garoufalidis and his Ph.D. advisor Don Zagier for enlightening discussions, as well as Francis Bonahon for helpful explanations regarding arborescent links. Part of this work appeared in [49]. The authors were partially funded by the Irish Research Council Advanced Laureate Award IRCLA/2023/1934. The second author was also partially supported by the Max-Planck-Gesellschaft.

REFERENCES

- [1] C. Adams, E. Flapan, A. Henrich, L.H. Kauffman, L.D. Ludwig and S. Nelson, *Encyclopedia of knot theory*, CRC Press, Boca Raton, FL, 2021.
- [2] G.E. Andrews, *An analytic generalization of the Rogers-Ramanujan identities for odd moduli*, Proc. Nat. Acad. Sci. U.S.A. **71** (1974), 4082–4085.

- [3] G.E. Andrews, *Knots and q -series*, Ramanujan 125, 17–24. Contemp. Math., **627** American Mathematical Society, Providence, RI, 2014.
- [4] C. Armond, *The head and tail conjecture for alternating knots*, Algebr. Geom. Topol. **13** (2013), no. 5, 2809–2826.
- [5] C. Armond, O.T. Dasbach, *Rogers-Ramanujan type identities and the head and tail of the colored Jones polynomial*, preprint available at <https://arxiv.org/abs/1106.3948>
- [6] C. Armond, O.T. Dasbach, *The head and tail of the colored Jones polynomial for adequate knots*, Proc. Amer. Math. Soc. **145** (2017), no. 3, 1357–1367.
- [7] P. Beirne, *On the 2-head of the colored Jones polynomial for pretzel knots*, Q. J. Math. **70** (2019), no. 4, 1353–1370.
- [8] P. Beirne, R. Osburn, *q -series and tails of colored Jones polynomials*, Indag. Math. (N.S.) **28** (2017), no. 1, 247–260.
- [9] S. Bettin, S. Drappeau, *Modularity and value distribution of quantum invariants of hyperbolic knots*, Math. Ann. **382** (2022), no. 3–4, 1631–1679.
- [10] F. Bonahon, L. Siebenmann, *New geometric splittings of classical knots, and the classification and symmetries of arborescent knots*, preprint available at <https://dornsife.usc.edu/francis-bonahon/wp-content/uploads/sites/205/2023/06/BonSieb-compressed.pdf>
- [11] J. Bruinier, G. van der Geer, G. Harder and D. Zagier, *The 1-2-3 of modular forms*, Universitext, Springer-Verlag, Berlin, 2008.
- [12] F. Calegari, S. Garoufalidis and D. Zagier, *Bloch groups, algebraic K -theory, units, and Nahm’s conjecture*, Ann. Sci. Éc. Norm. Supér. (4) **56** (2023), no. 2, 383–426.
- [13] A. Caudron, *Classification des nœuds et des enlacements*, Publ. Math. Orsay **82**, 4, Université de Paris-Sud, Département de Mathématiques, Orsay, 1982.
- [14] J.H. Conway, *An enumeration of knots and links, and some of their algebraic properties*, Computational Problems in Abstract Algebra (Proc. Conf., Oxford, 1967), pp. 329–358, Pergamon Press, Oxford-New York-Toronto, Ont., 1970.
- [15] O.T. Dasbach, X.-S. Lin, *On the head and tail of the colored Jones polynomial*, Compos. Math. **142** (2006), no. 5, 1332–1342.
- [16] M. Elhamdadi, M. Hajij, *Pretzel knots and q -series*, Osaka J. Math. **54** (2017), no. 2, 363–381.
- [17] M. Elhamdadi, M. Hajij, *Foundations of the colored Jones polynomial of singular knots*, Bull. Korean Math. Soc. **55** (2018), no. 3, 937–956.
- [18] M. Elhamdadi, M. Hajij and M. Saito, *Twist regions and coefficients stability of the colored Jones polynomial*, Trans. Amer. Math. Soc. **370** (2018), no. 7, 5155–5177.
- [19] M. Elhamdadi, M. Hajij and J. Levitt, *q -series and quantum spin networks*, J. Topol. Anal. **14** (2022), no. 3, 709–727.
- [20] D. Gabai, *Genera of the arborescent links*, Mem. Amer. Math. Soc. **59** (1986), no. 339, i–viii and 1–98.
- [21] S. Garoufalidis, T. Lê, *Nahm sums, stability and the colored Jones polynomial*, Res. Math. Sci. **2** (2015), Art. 1, 55 pp.
- [22] S. Garoufalidis, D. Zagier, *Asymptotics of Nahm sums at roots of unity*, Ramanujan J. **55** (2021), no. 1, 219–238.
- [23] S. Garoufalidis, D. Zagier, *Knots and their related q -series*, SIGMA Symmetry Integrability Geom. Methods Appl. **19** (2023), Paper No. 082, 39 pp.
- [24] S. Garoufalidis, D. Zagier, *Knots, perturbative series and quantum modularity*, SIGMA Symmetry Integrability Geom. Methods Appl. **20** (2024), Paper No. 055, 87 pp.
- [25] A. Goswami, R. Osburn, *Quantum modularity of partial theta series with periodic coefficients*, Forum Math. **33** (2021), no. 2, 451–463.
- [26] B. Gren, J. Sulkowska and B. Gabrovšek, *Classification of algebraic tangles*, preprint available at <https://arxiv.org/abs/2504.06901>
- [27] M. Hajij, *The Bubble skein element and applications*, J. Knot Theory Ramifications **23** (2014), no. 14, 1450076, 30 pp.
- [28] M. Hajij, *The tail of a quantum spin network*, Ramanujan J. **40** (2016), no. 1, 135–176.
- [29] M. Hajij, *The colored Kauffman skein relation and the head and tail of the colored Jones polynomial*, J. Knot Theory Ramifications **26** (2017), no. 3, 1741002, 14 pp.

- [30] K. Hall, *Higher order stability in the coefficients of the colored Jones polynomial*, J. Knot Theory Ramifications **27** (2018), no. 3, 1840010, 26 pp.
- [31] K. Hikami, S. Sugimoto, *Torus links $T_{2s,2t}$ and (s,t) -log VOA*, preprint available at <https://arxiv.org/abs/2306.03338>
- [32] S. Kanade, *Coloured \mathfrak{sl}_r invariants of torus knots and characters of \mathcal{W}_r algebras*, Lett. Math. Phys. **113** (2023), no. 1, Paper No. 5, 21 pp.
- [33] S. Kanade, *Characters of logarithmic vertex operator algebras and coloured invariants of torus links*, Proc. Amer. Math. Soc. Ser. B. **11** (2024), 157–172.
- [34] S. Kanade, *Coloured invariants of torus knots, \mathcal{W} algebras, and relative asymptotic weight multiplicities*, Comm. Math. Phys. **405** (2024), no. 11, Paper No. 257, 31 pp.
- [35] R.M. Kashaev, *The hyperbolic volume of knots from the quantum dilogarithm*, Lett. Math. Phys. **39** (1997) no. 3, 269–275.
- [36] K. Kawasoe, *The one-row-colored \mathfrak{sl}_3 Jones polynomials for pretzel links*, J. Knot Theory Ramifications **32** (2023), no. 1, Paper No. 2250105, 45 pp.
- [37] A. Keilthly, R. Osburn, *Rogers-Ramanujan type identities for alternating knots*, J. Number Theory **161** (2016), 255–280.
- [38] R.J. Lawrence, D. Zagier, *Modular forms and quantum invariants of 3-manifolds*, Asian J. Math. **3** (1999), no. 1, 93–107.
- [39] C. Lee, *A trivial tail homology for non-A-adequate links*, Algebr. Geom. Topol. **18**, no. 3, 1481–1513.
- [40] C. Lee, *Stability properties of the colored Jones polynomial*, J. Knot Theory Ramifications **28** (2019), no. 8, 1950050, 20 pp.
- [41] C. Lee, R. van der Veen, *Colored Jones polynomials without tails*, Algebr. Geom. Topol. **22** (2022), no. 6, 2857–2865.
- [42] H. Murakami, *An introduction to the volume conjecture*, Interactions between hyperbolic geometry, quantum topology and number theory, 1–40, Contemp. Math., **541**, Amer. Math. Soc., Providence, RI, 2011.
- [43] H. Murakami, J. Murakami, *The colored Jones polynomials and the simplicial volume of a knot*, Acta Math. **186** (2001), no. 1, 85–104.
- [44] H. Murakami, J. Murakami, M. Okamoto, T. Takata and Y. Yokota, *Kashaev’s conjecture and the Chern-Simons invariants of knots and links*, Experiment. Math. **11** (2002), no. 3, 427–435.
- [45] H. Murakami, Y. Yokota, *Volume conjecture for knots*, SpringerBriefs Math. Phys., 30, Springer, Singapore, 2018.
- [46] J. Murakami, *Complexified tetrahedrons, fundamental groups, and volume conjecture for double twist knots*, preprint available at <https://arxiv.org/abs/2501.00225>
- [47] W. Nahm, *Conformal field theory and torsion elements of the Bloch group*, Frontiers in number theory, physics, and geometry. II, 67–132, Springer, Berlin, 2007.
- [48] L. Rozansky, *Khovanov homology of a unicolored B-adequate link has a tail*, Quantum Topol. **5** (2014), no. 4, 541–579.
- [49] M. Storzer, *q-series, their modularity, and Nahm’s conjecture*, Ph.D. thesis, University of Bonn, 2024.
- [50] M. Vlasenko, S. Zwegers, *Nahm’s conjecture: asymptotic computations and counterexamples*, Commun. Number Theory Phys. **5** (2011), no. 3, 617–642.
- [51] C. Wheeler, *Quantum modularity for a closed hyperbolic 3-manifold*, SIGMA Symmetry Integrability Geom. Methods Appl. **21** (2025), Paper No. 004, 74 pp.
- [52] M. Willis, *A colored Khovanov spectrum and its tail for B-adequate links*, Algebr. Geom. Topol. **18** (2018), no. 3, 1411–1459.
- [53] T. Yang, *Recent progresses on the volume conjecture for Reshetikhin-Turaev and Turaev-Viro invariants*, Acta Math. Vietnam. **46** (2021), no. 2, 389–398.
- [54] W. Yuasa, *A q-series identity via the \mathfrak{sl}_3 colored Jones polynomial for the $(2,2m)$ -torus link*, Proc. Amer. Math. Soc. **146** (2018), no. 7, 3153–3166.
- [55] W. Yuasa, *Twist formulas for one-row colored A_2 webs and \mathfrak{sl}_3 -tails of $(2,2m)$ -torus links*, Acta Math. Vietnam. **46** (2021), no. 2, 369–387.
- [56] D. Zagier, *The dilogarithm function*, Frontiers in number theory, physics, and geometry. II, 3–65, Springer-Verlag, Berlin, 2007.

- [57] D. Zagier, *Quantum modular forms*, Quanta of maths, 659–675, Clay Math. Proc., **11**, Amer. Math. Soc., Providence, RI, 2010.

SCHOOL OF MATHEMATICS AND STATISTICS, UNIVERSITY COLLEGE DUBLIN, BELFIELD, DUBLIN 4, IRELAND

Email address: `robert.osburn@ucd.ie`

Email address: `matthias.storzer@ucd.ie`